Molecular π pulses: Population inversion with positively chirped short pulses

Jianshu Cao,[a] Christopher J. Bardeen,[b] and Kent R. Wilson
Department of Chemistry and Biochemistry, University of California, San Diego, La Jolla, California 92093-0339

(Received 26 May 1998; accepted 5 May 2000)

Detailed theoretical analysis and numerical simulation indicate that nearly complete electronic population inversion of molecular systems can be achieved with intense positively chirped broadband laser pulses. To provide a simple physical picture, a two-level model is used to examine the condition for the so-called π pulses and a four-level model is designed to demonstrate for molecular systems the correlation between the sign of the chirp and the excited state population. The proposed molecular π pulse is the combined result of vibrational coherence in the femtosecond regime and adiabatic inversion in the picosecond regime. Numerical results for a displaced oscillator, for LiH and for I_2, show that the proposed molecular π pulse scheme is robust with respect to changes in field parameters such as the linear positive chirp rate, field intensity, bandwidth, and carrier frequency, and is stable with respect to thermal and condensed phase conditions including molecular rotation, rovibronic coupling, and electronic dephasing. © *2000 American Institute of Physics.* [S0021-9606(00)02129-2]

I. INTRODUCTION

The production of desired nonequilibrium molecular distributions is the ultimate goal of much of chemistry. One such unusual distribution is a molecular system with population only on a high-lying electronic excited state inaccessible by thermal fluctuations. Such an electronically inverted molecular system defies the canonical Boltzmann distribution and formally defines a negative temperature. From this highly nonequilibrium distribution, chemical reactions and physical processes can proceed with a quantum efficiency impossible to achieve otherwise. Population inversion is well-known as one of the working principles of lasers.

With advances in theoretical understanding and laser technology, selective optical excitation holds great promise for controlling chemical systems.[1–9] In a simplistic picture, each electronic transition in a molecule is approximated by a two-level system, which can be completely inverted by a resonant π pulse. The canonical solution for a two-level system interacting with a resonant pulse exhibits the so-called Rabi oscillation,[10] which is determined by the product of light-matter coupling strength, pulse duration, and field strength. Complete inversion takes place when the pulse is on resonance and satisfies a constant area condition, the π pulse condition. However, multiple optical transitions with different coupling strengths and frequencies in real molecular systems make it impossible to define a single π pulse which is in resonance with all transitions and which simultaneously satisfies the area condition for each transition. Assuming a random distribution of transitions, one is as likely to find complete inversion of one transition as to find complete back transfer for another transition, as well as any other probability in between. Consequently, on average, the saturation for transform-limited pulses consists of half the probability on the ground state and half on the excited state, resulting in an inversion probability of about 50%. Therefore, it is a challenge to find a general π pulse which completely inverts molecular systems.

Along with the production of short intense pulses, various techniques have been developed to modulate and even ''shape'' laser pulses. The most exploited feature of modulated pulses is the chirp, which describes the temporal variation of the carrier frequency.[11–16] If the frequency increases with time, the pulse is positively chirped; if the frequency decreases with time, the pulse is negatively chirped. As will become evident, the chirp proves to be crucial in achieving complete inversion of molecular systems. It is well-known that complete population inversion can be accomplished through adiabatic passage, where the laser frequency sweeps from and to far off-resonance, i.e., from below to above or from above to below. The technique has been successfully applied to three-level systems by Bergmann and co-workers,[11] and to more complicated level systems by Kobrak and Rice.[16] Using linearly chirped picosecond pulses, Warren and co-workers successfully demonstrated the feasibility of adiabatic inversion in I_2 vapor.[13] Meanwhile, in an early numerical simulation, Ruhman and Kosloff showed that negatively chirped pulses are more efficient than their unchirped counterparts for generating large-amplitude vibrational motion on the ground electronic state surface of CsI through an effective intrapulse pump–dump mechanism.[17] Following this numerical study, Cerullo *et al.*[18] observed strong chirp dependence for high-power femtosecond pulse excitation of dye molecules in solution, and found that the

[a]Present address: Department of Chemistry, Massachusetts Institute of Technology, 77 Mass. Ave., Cambridge, MA 02139.
[b]Present address: Box 20-6 CLSL, Department of Chemistry, University of Illinois, 600 S. Mathews Ave., Urbana, IL 61801.

intrapulse pump–dump process is enhanced by negatively chirped pulses and suppressed by positively chirped pulses. In a sense, this intrapulse pump–dump process corresponds exactly to population back transfer, the reverse process of population inversion. Thus, based on the above two studies, it is reasonable to consider the generality of population control using positively chirped intense laser pulses. In fact, based on the previous studies, we have recently proposed and demonstrated molecular π pulses for complete inversion of molecular systems.[19,9] However, many questions remain such as to what degree the molecular population is inverted, what factors determine the inversion probability, and how stable and robust is the inversion mechanism. In this paper, we analyze these problems in more depth.

Theoretical aspects of population inversion have been explored earlier along different lines.[20–23] Making use of displaced harmonic oscillator potentials, Somloi, Lorincz, and Rice[20,21] obtained the resonance condition for pulses much shorter than the time scale of vibrational motion and found that in this limit the displaced harmonic oscillator system responds to intense laser pulses as a two-level system. For relatively longer pulses, the concept of a π pulse is not well defined and optimal control theory becomes the method of choice for maximizing population inversion. The idea of designing an optimal laser field to drive a quantum system to a specific target has stirred a surge of theoretical and experimental interest. In practice, the laser fields thus obtained often contain complicated phase and amplitude structures which can only be produced with sophisticated pulse-shaping techniques. Though a powerful mathematical tool, optimal control theory does not necessarily provide a direct route to understanding the general principle of the underlying physics, which can often be interpreted with the help of simple arguments and pictures. In fact, as demonstrated in this paper and the previous theoretical paper,[19] electronic population inversion turns out to be an advantageous case for which arguments derived from simple models prove to be sufficient and robust. For other more complicated processes, a general approach combining optimal control theory and a feedback mechanism may provide the ultimate solution.[3,9]

The present paper is organized as follows. In Sec. II A, a general resonant π pulse condition is derived by adopting the coordinate-dependent two-level approximation in the short-pulse limit. In Sec. II B, a novel four-level model is constructed to show that positively chirped pulses are the most efficient in population transfer. Then, the vibrational coherence induced by a femtosecond laser is explored in Sec. II C, which leads to the possibility of complete population inversion using intense positively chirped broadband pulses and the existence of the optimal intrapulse pump–dump process using negatively chirped pulses. Finally, in Sec. II D, conditions for adiabatic inversion are examined and a combination of the adiabatic and coherent effects in the picosecond regime is suggested. In Sec. III, numerical results for a displaced harmonic oscillator system and for LiH and I_2 are presented, which not only verify the theoretical models presented in Sec. II, but also demonstrate the stability and reliability of complete inversion with positive chirp in many realistic scenarios. Further discussions in Sec. IV conclude the paper. In the Appendix, we present a simple algorithm to introduce electronic dephasing on the wave function level.

II. ANALYSIS OF MOLECULAR π PULSES

We briefly review the general formalism of a molecular system interacting with a laser field through a dipole interaction. For simplicity, the molecular system consists of two electronic states, $|g\rangle$ and $|e\rangle$, described by two diabatic nuclear Hamiltonians, $\hat{H}_g$ for the ground state and $(\hat{H}_e + \hbar\omega_{eg})$ for the excited state. The electric field is treated classically as $\epsilon(t)=E(t)+E^*(t)=2\Re E(t)$, with $\Re$ indicating the real part. Within the rotating wave approximation, the total Hamiltonian is given as

$$\hat{H}(t)=\hat{H}_M+\hat{H}_{\rm int}, \tag{1}$$

where the molecular term is $\hat{H}_M=\hat{H}_g|g\rangle\langle g|+[\hat{H}_e+\omega_{eg}-\omega(t)]|e\rangle\langle e|$, with ω_{eg} being the transition frequency between the two states, and the interaction term is $\hat{H}_{\rm int}=-\mu E^*(t)|g\rangle\langle e|-\mu E(t)|e\rangle\langle g|$, with μ being the transition dipole moment.

To facilitate theoretical analysis, we define a Gaussian pulse as

$$E(t)=E_0\exp\left[-\frac{(t-t_0)^2}{2\tau^2}-i\omega_0(t-t_0)-ic\frac{(t-t_0)^2}{2}\right], \tag{2}$$

where E_0, ω_0, t_0, τ, and c are the amplitude, carrier frequency, temporal center, temporal width, and linear chirp rate, respectively, and where the complex conjugate part of the field is ignored under the rotating wave approximation. Taking the Fourier transformation of the field, we obtain the power spectrum as $P(\omega)=|\tilde{E}(\omega)|^2=|\tilde{E}_0|^2[-(\omega-\omega_0)^2/\Gamma^2]$, where the bandwidth is given as $\Gamma^2=c^2\tau^2+1/\tau^2$, and $\tilde{E}(\omega)$ is defined below. Here, by definition, the pulse duration is related to the full width half maximum of the temporal intensity profile by $\Delta t_{\rm FWHM}=2\tau\sqrt{\ln 2}$, and the bandwidth is related to the full width half maximum of the power spectrum by $\Delta\omega_{\rm FWHM}=2\Gamma\sqrt{\ln 2}$. The chirp describes the correlation between frequency and time, which cannot be deduced from the intensity versus time or the intensity versus frequency, i.e., the power spectrum. The Gaussian pulse in Eq. (2) can also be defined in the frequency domain as

$$\tilde{E}(\omega)=\tilde{E}_0\exp\left[-\frac{(\omega-w_0)^2}{2\Gamma^2}-ic'\frac{(\omega-w_0)^2}{2}\right], \tag{3}$$

where c' is the linear chirp rate in the frequency domain. Fourier transforming the field back to the time domain, we have the temporal profile of the intensity $P(t)=|E_0|^2\exp[-(t-t_0)^2/\tau^2]$, where the pulse duration is given as $\tau^2=1/\Gamma^2+c'^2\Gamma^2$. In addition, two identities can be established between the time domain and frequency domain parameters: $\Gamma^2c'=\tau^2c$ and $\Gamma|\tilde{E}_0|^2=2\pi\tau|E_0|^2$. For the theoretical analysis of intense short pulses, the time domain representation is more convenient, as the so-called Rabi oscillation is observed in real time. However, in a realistic experimental

situation, the chirp is usually adjusted for a fixed spectrum, and thereby the frequency domain representation is often more relevant.

In addition to the Gaussian pulse, another useful functional form is the square pulse, for which the phase and amplitude in Eq. (1) are defined as

$$\omega(t)=\omega_0+c(t-\tau/2) \tag{4}$$

and

$$A(t)=E_0[\theta(t)-\theta(t-\tau)], \tag{5}$$

where $\theta(t)$ is the step function. The square functional form introduces a sharp rise and fall at $t=0$ and $t=\tau$, which can be smoothed out by adding softer boundary conditions. Though in reality laser pulses are neither Gaussian nor square, the set of electric field parameters introduced above characterizes the basic features of laser fields, and thus the conclusions presented below are valid in general.

The population inversion problem is described as the following: After the excitation by an electric field fulfilling the π pulse conditions, the population of a molecular system initially on the ground electronic state can be completely transferred to the excited electronic state. The question we will address is what general laser pulse characteristics can lead to optimal population inversion regardless of the details of the potential energy surfaces or the initial molecular configuration.[19] In particular, effects due to linear chirp are examined in detail.

A. Impulsive excitation: Two-level model

Atoms and molecular systems with frozen nuclear configurations can be effectively modeled as a two-level system (TLS).[24,15] For simplicity, consider a two-level atom coupled to a transform limited square pulse as defined in Eqs. (4) and (5) with $c=0$. Then, the inversion probability, namely the excited state population, can be expressed in a closed form as

$$P_e=\frac{\Omega_0^2}{\Omega^2}\sin^2[\Omega\tau], \tag{6}$$

where Ω_0 is the resonant Rabi frequency, $\Omega_0=\mu E_0/\hbar$, and Ω is the off-resonant Rabi frequency $\Omega^2=\Omega_0^2+(\omega_0-\omega_{eg})^2$. It then follows that the maximum population transfer can be achieved under the constant area condition for a π pulse, $\Omega\tau=\pi/2$. When on resonance, a π pulse inverts all the population from the ground state to the excited state.

For a molecular system, the two atomic levels in the two-level model become two multidimensional electronic potential energy surfaces as described by Eq. (1). Consequently, there exists a large number of transitions between the two electronic manifolds, and a vibronic state on one electronic surface can be coupled to more than one vibronic state on the other surface. As a result, one cannot define a simple π pulse condition which is universally satisfied by all pairs of transitions in a molecular system and, therefore, cannot achieve population inversion based on the simple argument developed for two-level systems.

Nevertheless, if the pulse duration is sufficiently shorter than the characteristic vibrational period on the electronic surfaces, the nuclear motion of a molecular system can be considered frozen during the process. This approach ignores the kinetic energy operator in Eq. (1) and leads to a coordinate-dependent two-level model. Recently, we examined the validity of the assumption and subsequently extended the model to a nonstationary wave packet in pump–probe and multiphoton experiments.[15,25] By virtue of this approximation, the excited population can be written as

$$P_e=\left\langle \frac{\Omega_0^2}{\Omega^2(x)}\sin^2[\Omega(x)\tau]\right\rangle_g, \tag{7}$$

where $\langle\cdots\rangle_g$ denotes an average over the ground-state distribution $\rho_g(x)$ and $\Omega(x)$ denotes the coordinate-dependent Rabi frequency defined as $\Omega^2(x)=\Omega_0^2+[\omega_0-\omega_{eg}(x)]^2$, with the vertical transition frequency $\omega(x)=\omega_{eg}+[V_e(x)-V_g(x)]/\hbar$. The time-dependent factor in the integrand of Eq. (7) can be expanded as

$$\sin^2[\Omega(x)\tau]=\sin^2(\Omega_0\tau)+\sin(2\Omega_0\tau)[\Omega(x)-\Omega_0]\tau+\cdots, \tag{8}$$

which converges if

$$\langle[\Omega(x)-\Omega_0]\rangle_g\tau\leqslant 1, \tag{9}$$

indicating an upper bound for the pulse duration. The leading term in Eq. (9) is $\langle\omega_{eg}^2(x)\rangle_g=\Omega_0^2$, which leads to the resonance condition for the molecular system, i.e.,

$$\omega_0=\omega_{eg}+\frac{V_e(x_0)-V_e(x_0)}{\hbar}, \tag{10}$$

where the ground-state distribution is assumed to peak at x_0. As expected, the resonant frequency is exactly the vertical transition frequency in the Franck–Condon regime. Then, a short intense π pulse which satisfies

$$\Omega_0\tau=\frac{\pi}{2} \tag{11}$$

can invert most of the ground-state population, implying a π pulse behavior for the molecular system in the short-time regime.[20,21]

In addition to the short pulse and resonance conditions, the high intensity of a π pulse is necessary to reduce the coordinate dependence in the time series of Eq. (8) and to maximize the prefactor $\Omega_0/\Omega(x)$ in Eq. (7), thus increasing the overall efficiency of population inversion. Since a π pulse is constrained by the area relation in Eq. (10), the short pulse duration and high field strength constitute a pair of consistent and correlated conditions for inverting molecular systems. To estimate the pulse duration, or equivalently the field strength, we expand the right-hand side of Eq. (9) and obtain the leading order correction to a π pulse as

$$\Gamma_a^2\tau\leqslant\Omega_0, \tag{12}$$

where the resonant condition in Eq. (10) is applied. Here, Γ_a is roughly the bandwidth of the absorption spectrum, explicitly expressed as $\Gamma_a^2=\langle[\omega_{eg}(x_0)-\omega_{eg}(x)]^2\rangle_g$, which is generally temperature dependent. Further, by use of the area relation in Eq. (11) for a π pulse and $\Gamma=1/\tau$ for a transform-limited pulse, Eq. (12) is simplified to

$$\Gamma\geqslant\Gamma_a, \tag{13}$$

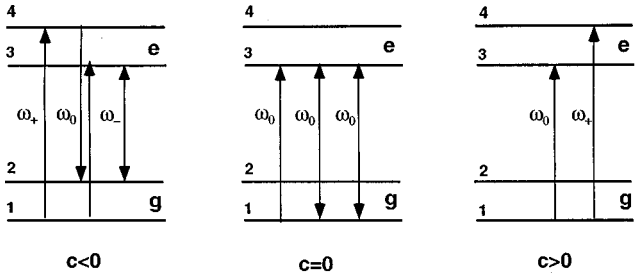

FIG. 1. Illustration of the four-level model discussed in Sec. II B. There are two vibronic levels on each of the ground and excited electronic states. Under the assumption that the energy gaps on the ground and excited surfaces are the same, there are three distinct transition frequencies ω_-, ω_0, and ω_+. The electric field is represented by a square pulse divided equally into three segments with the carrier frequencies assigned to each segment according to the chirp.

implying a broad bandwidth comparable to the absorption spectrum. Based on this relationship, for a typical π pulse to invert molecular systems, the bandwidth is hundreds of wave numbers, the duration is a few femtoseconds, and the intensity is $10^{13}-10^{15}\,\mathrm{W/cm^2}$. In this intensity range, the deviation from the two-electron-state model may become observable and hence population inversion may be complicated by other competitive processes such as multiphoton excitation and ionization, which are not desirable for population inversion.

As will be verified later on, we argue that the prerequisite for population inversion is the bandwidth requirement in Eq. (13) rather than the area relation in Eq. (11), which is valid only for short transform-limited pulses. Consequently, one way to avoid the relatively high intensity is to stretch the pulse duration by chirping, which according to the relations for the Gaussian pulses significantly reduces the field strength by increasing the pulse duration but still maintains the same power spectrum required by Eq. (13). In fact, by incorporating linear chirp, one introduces some exciting new physics unexpected from transform-limited pulses, which will be demonstrated in the following sections.

B. Coherent effect: Four-level model

The difficulty associated with two-level models for the optical excitation of a molecular system by a non-transform-limited pulse is twofold. First, there are no closed-form solutions for the two-level model in the presence of linear chirp. Second, the frozen wave packet approximation discussed earlier does not describe the coherent effect induced by the chirp of an optical pulse.

In order to understand the essence of the physics in a simple manner, we construct a novel model consisting of a four-level molecule interacting with a three-segment square pulse. Two vibronic eigenstates, $|1\rangle$ and $|2\rangle$, on the ground electronic surface, and similarly two vibronic eigenstates, $|3\rangle$ and $|4\rangle$, on the excited electronic surface, are included to describe the molecular system. Thus, there are three resonant frequencies (see Fig. 1): ω_- for the transition between $|2\rangle$ and $|3\rangle$; ω_+ for the transition between $|1\rangle$ and $|4\rangle$; and ω_0 for the transitions between $|1\rangle$ and $|3\rangle$ and between $|2\rangle$ and $|4\rangle$, assuming the energy gaps on the ground and excited electronic surfaces are the same. To represent a chirp, we divide a square pulse of duration 3τ equally into three segments, each of duration τ but with a different carrier frequency. For positive chirp, the sequence of the three segments is $\{\omega_-,\omega_0,\omega_+\}$; for zero chirp, the sequence is $\{\omega_0,\omega_0,\omega_0\}$; for negative chirp, the sequence is $\{\omega_+,\omega_0,\omega_-\}$. To simplify the analysis, we assume that the system is initially populated on the $|1\rangle$ state. Then, depending on the sign of the chirp, the three-segment pulse will be in resonance with various transitions in a specific order, shown schematically in Fig. 1. The sequence and order clearly demonstrate the coherent interplay between the phase coherence of light fields and molecular dynamics.

A general four-level system is a formidable problem to solve analytically. Fortunately, for the particular model described above, each segment of the pulse is resonant with one pair or two distinct pairs of transitions, so that the four-level problem can be decomposed into a sequence of two-level transitions if we ignore the contribution from off-resonant transitions. The wave function on the four levels can be followed by applying two-level propagation three times for each pulse section. Consequently, the excited state population can be evaluated, giving for a positive chirp

$$P_+=\sin^2(\phi)+\cos^2(\phi)\sin^2(\phi), \tag{14}$$

for the zero chirp

$$P_0=\sin^2(3\phi), \tag{15}$$

and for a negative chirp

$$P_-=\sin^2(\phi)\cos^2(\phi)+\sin^2(\phi)\cos^2(2\phi), \tag{16}$$

with $\phi=\tau\Omega_0$. Evidently, for any pulse duration, a positive chirp can always invert more population than a negative chirp. Averaging over a broad distribution of Rabi frequencies in a realistic molecular system, we obtain

$$P_+:P_0:P_-=\tfrac{5}{8}:\tfrac{4}{8}:\tfrac{3}{8}, \tag{17}$$

which clearly favors using an optical pulse of a positive chirp for population inversion. This conclusion remains the same when the energy gaps on the ground and excited states are different.

Though based on an oversimplified model of a molecular system interacting with a chirped optical pulse, the conclusion thus drawn has general implications: As long as the eigenenergy spectrum is bounded from below and the initial configuration assumes a normal distribution on the ground electronic surface, a positive-chirp pulse is more efficient for population inversion than a transform-limited or negative-chirp pulse.

C. Femtosecond pulses: Wave packet picture

Though the four-level model is valid qualitatively, the large number of vibronic eigenstates in realistic molecular systems makes it impractical to analyze such systems quantitatively from the eigenstate picture. Because a subpicosecond laser pulse induces a vibrational wave packet as a result of the coherent superposition of vibrational eigenstates, a classical-like wave packet picture is more convenient for describing molecular chirp effects. As illustrated in Fig. 2, a

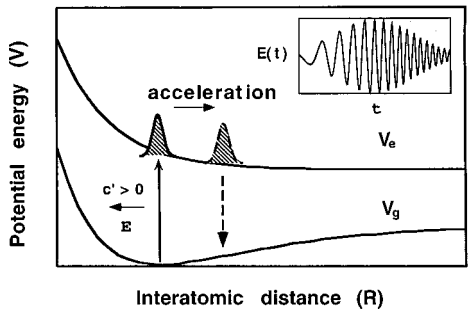

FIG. 2. Illustration of wave packet motion induced by a femtosecond pulse and its coupling to the chirped laser field. Optimal electronic state inversion occurs when the instantaneous peak photon energy is increasing with time (positive chirp, $c'>0$) while the resonant frequency $(V_e-V_g)/\hbar$ for the molecular wave packet is decreasing. The inset is a schematic positively chirped electric field.

short pulse couples to the part of the wave function located in a window where the vertical transition is resonant with the instantaneous frequency composition of the pulse. Since the ground-state distribution is in thermal equilibrium, the Franck–Condon region is relatively flat on the ground surface and steep on the excited surface. Thus, a positive chirp can always be in resonance with a wave packet moving upward on the excited surface and a negative chirp is resonant with a wave packet moving downward. Meanwhile, because of the nonstationary nature of the excited-state wave function, the initially excited wave packet gains momentum and accelerates downward. Consequently, by the time the Rabi oscillation starts to recycle the excited population back to the ground surface, a short laser pulse of sufficiently large positive chirp has become off-resonant with the moving wave packet. On the contrary, a negative chirp can follow the motion of the wave packet and hence recycle the excited electronic population back to the ground electronic state. Therefore, a positive chirp exploits the first phase of the Rabi oscillation to invert the population but avoids the second phase when the population is back transferred. Consequently, as the pulse duration increases, the excited-state population reaches a plateau instead of exhibiting a Rabi oscillation. It then follows from Eq. (13) that complete inversion requires a broad spectrum with sufficient intensity.

As indicated earlier, a negative chirp is effective in transferring the excited wave function back to the ground state, thus inducing wave packet motion in the initially stationary ground-state distribution. Here, we present a simple analysis to reveal the existence of an optimal linear chirp rate for transferring population back to the ground surface. For a short period of time t, the excited wave packet has moved to a distance of $\delta x \propto t^2 f/m$, with f the force and m the mass. During the same period, the central frequency has shifted $\delta\omega = ct$ which, by virtue of the coordinate-dependent two-level approximation, is proportional to the displacement of the wave function coupled to the pulse. The optimal chirp rate which follows the motion of the wave packet can be determined by $\delta\omega = -f\delta x/\hbar$, equivalently $c_{\mathrm{opt}} \propto -f^2 t/(m\hbar)$. Because back transfer becomes significant as the excitation process reaches maximum, a reasonable choice for t is taken from the π pulse condition in Eq. (11), which then leads to an estimate for the optimal linear chirp rate

$$c_{\mathrm{opt}} \propto -\frac{f^2}{mE_0}. \tag{18}$$

Though the situation is more complicated in reality, the above analysis provides a simple physical picture for the optimal negative chirp. In fact, the search for the optimal chirp can be posed as a strong field optimization problem and Eq. (18) can be verified numerically.

We can summarize pictorially, by thinking of how the color dynamics (how different colors follow one another in time) of the driving light pulse match or fail to match the color dynamics of the frequency receptivity of the driven molecular system. If they move in step, as with a negative chirp, we can pump up to the excited state and back down to the ground state. If they are out of step, as with a negative chirp, we can pump up, but not back down.

D. Picosecond pulses: Adiabatic inversion by frequency sweeping

In the above discussion, we have left out another important chirp effect: adiabatic population inversion, which becomes substantial in the picosecond time domain. An adiabatic process, by definition, involves a dynamical variable which changes sufficiently slowly compared to other time scales so that the system evolves according to an effective Hamiltonian in which the slowly varying variable is treated as a time-dependent parameter rather than as a dynamical variable. As an example, if the chirp-induced sweep is slow in comparison with the Rabi oscillation, the instantaneous frequency $\omega(t)$ can be considered as an adiabatic variable. Consequently, if the frequency sweep is far off resonance from one limit to the other, the adiabatic passage can switch the electronic states, giving rise to complete population inversion.

To be specific, consider a two-level atom coupled to a chirped square pulse, which under the rotating wave approximation can be described by Eqs. (1), (4), and (5) with constant Hamiltonians $\hat{H}_e$ and $\hat{H}_g$ and with the Rabi frequency $\Omega_0 = E\mu/\hbar$. If the initial optical frequency is far below resonance, i.e., $\omega_{eg} - \omega(0) \gg \Omega_0$, the initial adiabatic states of the interaction Hamiltonian in Eq. (1) are $\{|e\rangle, |g\rangle\}$ in the order of descending eigenvalues. Likewise, if the final optical frequency is far below resonance, i.e., $\omega(\tau) - \omega_{eg} \gg \Omega_0$, the final adiabatic states of the interaction Hamiltonian in Eq. (1) are $\{|g\rangle, |e\rangle\}$ in the order of descending eigenvalues. For the linear chirp defined by Eq. (4), the far-off resonance condition can be expressed as

$$c\tau > \Omega_0. \tag{19}$$

Note that, under this condition, the initial and final adiabatic states are the same as the electronic eigenstates but their orders are exchanged. To lock the eigenstates adiabatically, the change in the adiabatic eigenstates due to the frequency sweeping is smaller than the Rabi oscillation, i.e., $c < \Omega^2/\Omega_0$, which imposes an upper bound for the linear chirp rate,

$$\Omega_0^2 > c. \tag{20}$$

Then, adopting the adiabatic approximation and treating $\omega(t)$ as a parameter, the ground eigenstate can be adiabatically switched to the excited eigenstate and vice versa. Consequently, the population on the ground electronic state is completely transferred to the excited electronic state. The equalities in Eqs. (19) and (20) can be combined to give $\Omega_0/\tau < c < \Omega_0^2$, or

$$\Omega_0 \tau > 1, \tag{21}$$

which is related to the π pulse condition in Eq. (11). Because of the symmetry between the ground and excited states for a two-level atom, adiabatic inversion is independent of the sign of the chirp. For comparison, the coherent effect depends crucially on the sign of chirp, as previously demonstrated. Therefore, in principle, the two effects can be distinguished by changing the sign of chirp.

As pointed out earlier, a two-electronic-state molecule corresponds to a coupled multilevel system instead of a set of independent two-level systems. As a result, frequency sweeping can invert the population but can subsequently transfer the population back to the ground state through another transition. To invert population effectively, a large frequency sweep is required to satisfy the far-off-resonance condition to ensure adiabatic inversion, but at the same time a narrow spectral width is preferred to prevent back transfer. Therefore, the choice of the central frequency and the frequency sweep range becomes a subtle system-dependent issue in adiabatic inversion, as discussed by Warren and co-workers.[13]

From a different point of view, a two-electronic-state system can be treated as a generalized two-level problem with molecular Hamiltonians $\hat{H}_e$ and $\hat{H}_g$ as in Eq. (1). Following this line, we argue that if the energy gap between the vibronic eigenstates is considerably smaller than the electronic transition frequencies, and if the frequency sweeps from far below the lowest possible electronic transition to far above the highest possible electronic transition, the adiabatic eigenstates of the initial and final interaction Hamiltonian of Eq. (1) coincide with the molecular eigenstates and the inversion will be complete. In other words, if the electronic energy gap and the off-resonant sweep are large, the two-electronic-state molecule system becomes equivalent to an effective two-level atom. However, in theory, such a sweep is impossible because the vibronic transition frequency is not bounded from above. In practice, this implies that complete inversion requires a frequency sweep, typically on the order of the absorption spectral width, as indicated in Eq. (13). A more practical approach is to use positively chirped pulses in the intermediate regime from a few hundred femtoseconds to a few picoseconds, thus combining the advantages of adiabatic and coherent inversion. In this regime, positively chirped pulses remain the most favorable, whereas negatively chirped pulses become more effective than transform-limited pulses.

III. RESULTS

The theoretical analysis presented in the last section has clearly demonstrated the possibility of inverting molecular systems with positively chirped broadband laser pulses. Though simple analytical models such as the coordinate-dependent two-level approximation and the four-level molecule model reveal the underlying physics of population inversion, molecular systems in reality are complicated by numerous effects, including rovibronic coupling, selection rules for rotational levels, thermal population distribution, and electronic dephasing, and thereby can be fully investigated only through detailed numerical calculations. In addition, the calculated population inversion probability can be directly compared to experimental measurements, thus providing the ultimate test for our predictions based on simplified models. In the following, we present several example numerical results of strong-field nonperturbative quantum mechanics to confirm the molecular π pulse prediction.

A. Displaced harmonic oscillators

As the first example, the ground and excited electronic potentials are displaced harmonic oscillators described as $V_g(x) = m\omega^2 x^2/2$ and $V_e(x) = m\omega^2 (x-d)^2/2$, where ω, m, d are the frequency, mass, and displacement of the oscillators, respectively. For this model Hamiltonian, we assign dimensionless values for all parameters: $m=1$, $\hbar=1$, $\mu=1$, $\omega=1$, and $d=2$. Gaussian pulses as defined in Eqs. (2) and (3) are used with dimensionless units. To ensure accuracy, the wave function is represented on a fine spatial grid of 256 with cutoffs at $|x|_{\max}=6$ and is propagated via the fast Fourier transform at a time step of 0.02. The most important simplification involved in this model system is the assumption of harmonicity for the nuclear degree of freedom. Because the previous analysis does not invoke the harmonicity assumption, we do not expect anharmonicity to play a significant role in population inversion and therefore the results obtained from this model are generally applicable to anharmonic potential surfaces. In fact, exactly the same model has been used in two earlier studies of population inversion.[20,21] The results presented below represent an extensive investigation of this model and firmly establish the critical role of the chirp in population inversion.

Based on the analysis presented in the last section, the carrier frequency of laser pulses is set at $\omega_0=2$ according to the resonance condition in Eq. (10), and a bandwidth of $\Gamma=3$ is set to match the absorption spectrum. Since most experimental measurements are recorded for a given pulse spectral shape, it is reasonable to evaluate the population inversion probability as a function of linear frequency chirp rate c' and frequency domain field strength $\tilde{E}_0$ of the Gaussian pulse defined by Eq. (3). The inversion probability is the probability for the initially ground electronic state system to be on the excited electronic state after the pulse. The numerical results thus obtained are shown as a two-dimensional contour plot in Fig. 3. In the left end of the plot where the field is weak, straight vertical contour lines indicates chirp independence in the weak-response limit. As the field strength increases, the straight contour lines are deformed into differ-

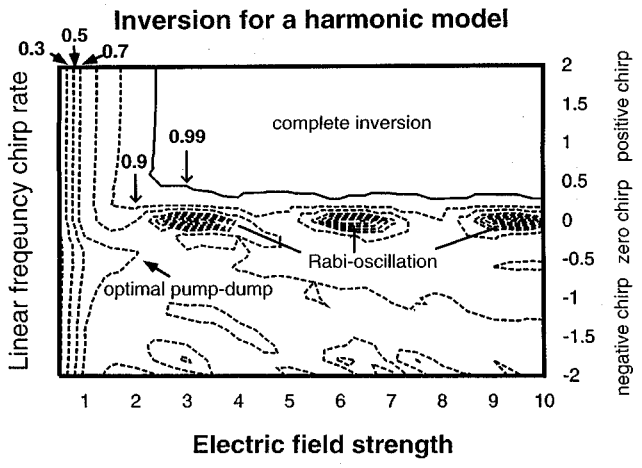

FIG. 3. Contour plot of inversion probability of the displaced harmonic oscillator defined in the text, as a function of linear frequency chirp rate and frequency domain peak electric field strength for a fixed bandwidth of $\Gamma=3$.

ent geometries. The rectangular domain in the upper part of the plot provides solid evidence of complete population inversion with positively chirped laser pulses and of the robustness of the solution with respect to a range of values of positive chirp and electric field strength. The two contour curves corresponding to 0.9 and 0.99 inversion probabilities strongly indicate that complete population inversion is universally accomplished once the field strength and positive chirp rate reach their critical values. Along the zero-chirp domain, three equally spaced valleys clearly show the well-known Rabi-oscillation behavior for transform-limited laser fields. The small islands in the lower part of the contour are the analog of the Rabi oscillation for negatively chirped pulses. The average inversion probability in this domain is below one half. The prominent peak of the curve along the field strength of about $\tilde{E}_0=1.0$ is the indication of the optimal intrapulse pump–dump process described approximately by Eq. (18), which induces maximum wave packet motion in the ground electronic state.

Next, we shall study the effect on population inversion of off-resonant detuning of the laser pulse. In Fig. 4, the

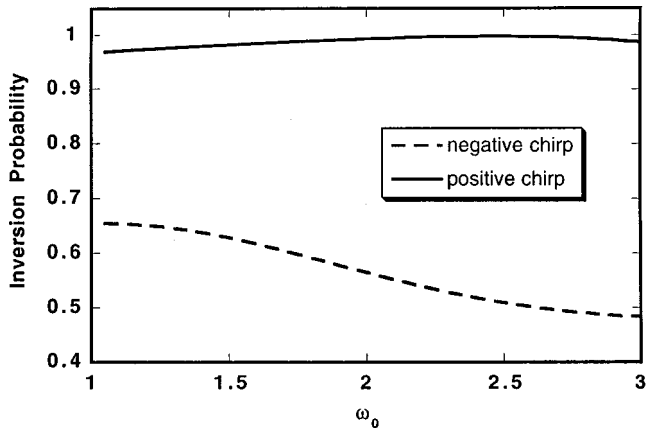

FIG. 4. Plot of the inversion probability of the displaced harmonic oscillator, defined in the text, as a function of central carrier frequency for $E=1.0$, $\tau=2$, and $c=\pm 1.0$.

inversion probability is plotted versus central frequency for a Gaussian pulse of $E_0=1.0$, $c=\pm 1.0$, and $\tau=2.0$. The carrier frequency is varied over roughly the bandwidth of the transition frequencies. Clearly, the large inversion probability of positively chirped pulses shows little response to the variation of the central frequency, whereas the negative chirped pulses appear to be more sensitive.

B. LiH

In this subsection, we study the $X(\Sigma^+)\rightarrow A(\Sigma^+)$ transition of LiH. The relatively light LiH system has appreciable quantum effects in nuclear motion and only a small number of rotational levels are thermally occupied with negligible population on the vibrational excited states at or below room temperature. We use *ab initio* data for the X and A potential energy surfaces and the transition dipole moment coupling them.[26] The LiH wave function is expanded as $\Sigma_{JM}R_JY_{JM}$, where the Y_{JM} are spherical harmonics and the R_J are the associated radial parts. Since each electronic transition changes from J to $J\pm 1$, the final range of the angular momentum distribution resulting form an initially pure J_0 state measures the degree of electronic excitation. In the simulation, J is truncated from J_0-10 to J_0+10 with J_0 being the initial J number. If J is smaller than 10, the range is adjusted to $J=0$ to $J=21$ so that the total number of the J states is always 21. The radial part of the wave function R_J is represented on a spatial grid of 256 points evenly spaced from 1.5 to 15.0 atomic units. Rotational effects including the rovibronic coupling are taken into full consideration and are treated exactly by nonperturbative quantum mechanics. A time step of 0.1 fs is used to propagate the wave function, through the fast Fourier transformation method.

Here again, the laser field is described by the Gaussian form of Eq. (2) or equivalently Eq. (3). The central frequency ω_0 is fixed at $\omega_0=29\,027\,\mathrm{cm}^{-1}$ according to the resonance condition in Eq. (10). A transform-limited pulse of 10 fs defines a bandwidth of 500 cm^{-1}, which is on the order of the absorption bandwidth as required by Eq. (13). By chirping the pulse, we can stretch the pulse duration and consequently reduce the peak intensity. To match the experimental conditions, c' is varied for a fixed power spectrum. For the given bandwidth Γ, by chirping the pulse, we increase the pulse duration according to $\tau^2=1/\Gamma^2+\Gamma^2c'^2$, change the temporal linear chirp rate by $c=c'\Gamma^2/\tau^2$, and decrease the peak intensity, because the integrated intensity $I_0=\tau E_0^2$ is a conserved quantity. For example, when $c'=\pm 0.4\,\mathrm{fs/cm}^{-1}$,[27] the $\tau=10$ fs transform-limited pulse is stretched to a chirped $\tau=200$ fs pulse and accordingly the peak intensity is reduced by a factor of 20. In Fig. 5, the pulse duration τ (fs) and intensity $E_0^2\,(\mathrm{W/cm}^{-2})$ are plotted as functions of linear frequency chirp rate c', assuming a peak intensity of about $10^{12}\,\mathrm{W/cm}^{-2}$ for the 10 fs pulse.

The resulting inversion probability for LiH molecules is plotted in Fig. 6 as a function of c' for two values of peak intensity, $1\times 10^{11}\,\mathrm{W/cm}^{-2}$ and $5\times 10^{11}\,\mathrm{W/cm}^{-2}$, respectively. For simplicity, the initial state is assumed to be the ground vibrational, rotational, and electronic state, that is, $\nu=M=J=0$. As will be seen later on, the results remain

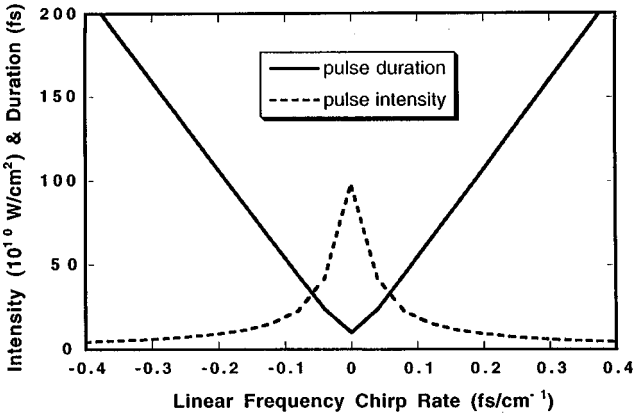

FIG. 5. Plot of the pulse duration τ (fs) and peak intensity I_0 (W/cm^{-2}) as functions of linear frequency chirp rate c' (fs/cm^{-1}) for a fixed power spectrum of $\Gamma=500$ cm^{-1}, $\omega_0=29\,027$ cm^{-1}, and $P_0=\tau E_0^2=10$ mJ/cm^2.

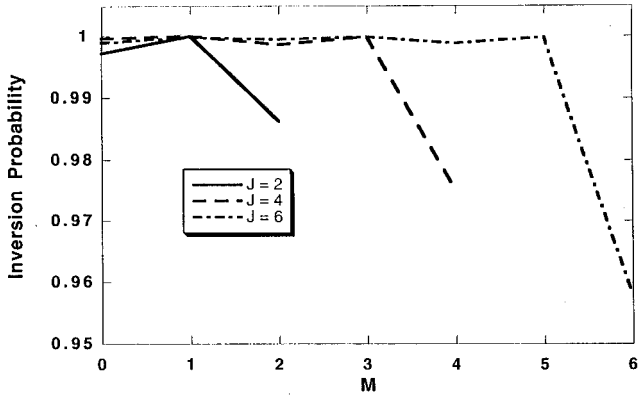

FIG. 7. Plot of LiH inversion probability as a function of M for $J=2$, 4, 6 under the constraint $M \leqslant J$. The Gaussian pulse parameters are taken as $E_0=2.5\times10^7$ V/cm, $I_0=8.3\times10^{11}$ W/cm^{-2}, $\tau=100$ fs, and $c'=5$ fs/cm^{-1}.

essentially the same when the system starts from different initial states. Similarly for the case of displaced harmonic oscillators, positive chirp consistently leads to high inversion probabilities, with complete inversion of over 99% for the higher intensity curve. As expected, the curve of $I_0=1\times10^{11}$ W/cm^{-2} is relatively flat and the curve of $I_0=5\times10^{11}$ W/cm^{-2} exhibits a sharp increase as a function of linear chirp rate c'. The first dip on the negative half of the plot can be interpreted as the optimal intrapulse pump–dump as explained in Sec. II C.

One challenge for inverting molecular systems is the thermal distribution on the ground electronic state surface, which gives rise to a broad distribution of Rabi frequency and transition frequency for inverting particular rovibronic pairs. Due to the relatively light mass of LiH, only a few vibrational and rotational levels on the ground electronic surface are accessible. The large value of the rotational constant B for LiH results in inhomogeneous broadening of the π pulse condition in Eq. (13). The effect due to the broadening of the Rabi frequency can be separated by studying the M dependence of the inversion probability for the same J quantum number, because the eigenenergy is independent of M, whereas the effective electronic dipole coupling varies with M. In Fig. 7, the inversion probability is plotted as a function of M for three values of J under the constraint $M \leqslant J$. The pulse parameters are taken as $E_0=2.5\times10^7$ W/cm^{-2}, $I_0=8.3\times10^{11}$ W/cm^{-2}, $\tau=100$ fs, and $c'=5$ fs/cm^{-1}. Clearly, complete inversion is sustained for all M numbers except for the case of $M=J$, for which the coupling drops significantly. Nevertheless, considering the range of inversion probability, a few percent change for a substate will not spoil the overall performance of the molecular π pulse. This statement is then verified by Fig. 8, where the inversion probability averaged over the possible $2J+1$ values of M is plotted as a function of J for the ground and first excited vibrational states. Overall high inversion probability is maintained for all J numbers, though there is a slight decrease near $J=7$ for $v=1$. This is caused by the large transition frequency which approaches the edge of the chosen pulse spectrum. Since complete inversion takes place almost equally for each eigenstate, and the thermal rate is an ensemble average of eigenstates according to the Boltzmann

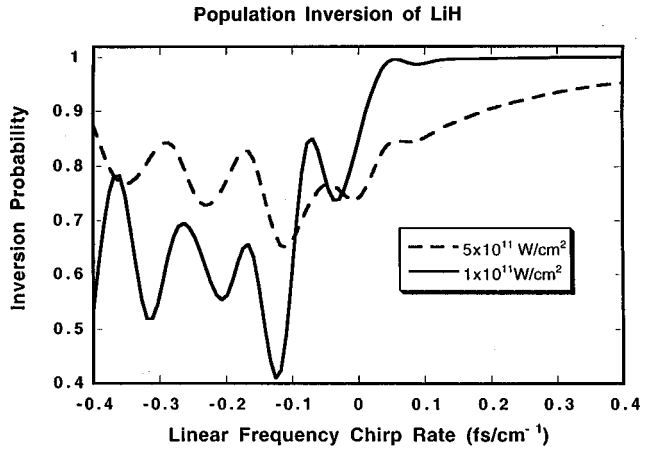

FIG. 6. Plot of the inversion probability of LiH as a function of linear frequency chirp rate for peak intensity $I_0=1\times10^{11}$ W/cm^{-2} and $I_0=5\times10^{11}$ W/cm^{-2}. The peak intensity is labeled for the ±0.4 fs/cm^{-1} linear frequency chirp rate and varies with the chirp rate as shown in Fig. 5.

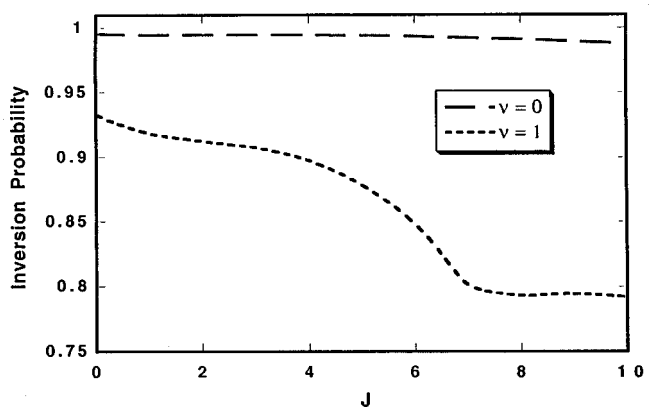

FIG. 8. Plot of LiH inversion probability averaged over the possible $2J+1$ values of M as a function of J for the ground and first excited vibrational states with the same Gaussian pulse as in Fig. 7.

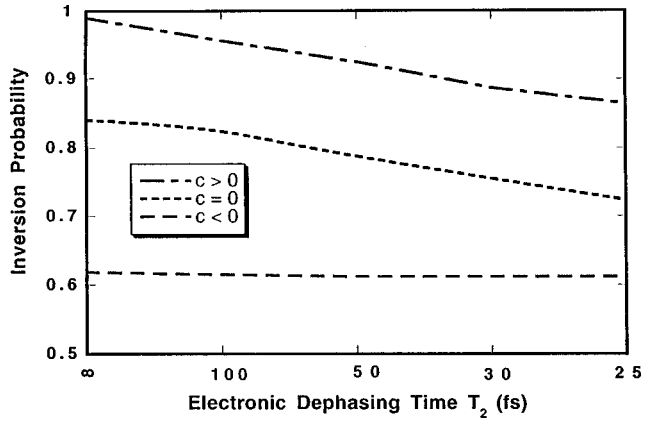

FIG. 9. Plot of the inversion probability for LiH as a function of electronic dephasing time T_2. The three curves are the results for pulses of the same bandwidth but with $\tau=50$ fs, $c'=0.05$ fs/cm^{-1}, $E_0=4\times10^7$ V/cm for the positive chirp curve; $\tau=5$ fs, $c'=0$ fs/cm^{-1}, $E_0=12.6\times10^7$ V/cm for the zero chirp curve; $\tau=50$ fs, $c'=-0.05$ fs/cm^{-1}, $E_0=4\times10^7$ V/cm for the negative chirp curve.

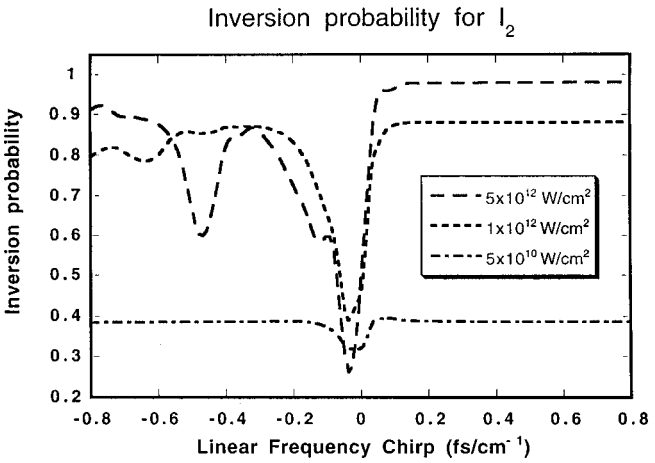

FIG. 10. Plot of the inversion probability of I_2 as a function of linear frequency chirp rate for a fixed power spectrum with 5×10^{10}, 1×10^{12}, and 5×10^{12} W/cm^{-2}, respectively. The peak intensity is labeled for the ±0.8 fs/cm^{-1} linear frequency chirp rate and varies with the chirp rate.

distribution, population inversion can be achieved over a wide range of temperatures. In the study of population inversion of I_2 gas below, we also find the inversion probability is stable with respect to changes in the vibrational quantum number.

To account for condensed phase environments, we now include electronic dephasing in the calculation. Electronic dephasing describes the fluctuations of the electronic transition frequency which varies on a time scale determined by the dephasing time T_2. In the Appendix, we introduce a numerical method to reproduce electronic dephasing on the wave function level. Since the dephasing process represents the fastest relaxation mechanism in a condensed phase environment, it is the most likely to have a significant effect on population transfer. In Fig. 9, the inversion probability is given as a function of T_2 for positive, zero, and negative chirp. No substantial loss of excited state population is observed until the dephasing time becomes smaller than the pulse duration. This result suggests that population inversion should be accomplished before phase coherence is lost.

C. I_2

As the final example, we study the $X\rightarrow B$ transition of gas phase I_2 molecules. In contrast to LiH, the heavier I_2 has a broad distribution of rotational states and can easily access vibrationally excited states at room temperature. Thus, it is a better example to study the effect of thermal distribution on population inversion. The disadvantage of I_2 is the relatively small transition dipole moment in comparison to LiH, which requires a considerably higher field intensity to achieve complete inversion even when a moderate positive chirp is applied. Consequently, to avoid various higher order optical processes induced by intense laser fields, large linear chirp rates are used to stretch the pulse duration close to the picosecond regime, such that the adiabatic mechanism discussed in Sec. II D become substantial. As a result, gas phase I_2 is a good example for studying various population inversion mechanisms ranging from impulsive excitation, to vibrational motion, to adiabatic passage.

To model gas phase I_2, Morse potentials are used to describe the X and B state surfaces[28] and the transition dipole is taken as a constant $\mu=0.181$ atomic units. Similarly, the rotational quantum number J is truncated from J_0-10 to J_0+10 with J_0 being the initial J number. If J is smaller than 10, the range is adjusted to $J=0$ to $J=21$ so that the total number of the J states remains 21. The radial part of the wave function is represented on a spatial grid of 256 points evenly spaced from 4 to 10 atomic units. A time step of 0.5 fs was used to propagate the wave function through the fast Fourier transform method. The Gaussian functional form in Eq. (2) is assumed with the central frequency at $\omega=19\,383$ cm^{-1} and with a bandwidth of 500 cm^{-1}, which corresponds to a 10 fs pulse transform-limited pulse. The pulse duration described increases from 10 fs for transform-limited pulses to 0.4 ps with a linear chirp rate of ±0.8 fs/cm^{-1}.

In Fig. 10, the inversion probability is plotted as a function of the frequency chirp c' at three different peak intensities of 5×10^{12}, 1×10^{12}, and 5×10^{10} W/cm^{-2}, respectively. For simplicity, the initial state is assumed to be $J=M=0$ of the ground vibration level on the ground electronic surface. As will become clear later, the assumption does not change the conclusions in a qualitative fashion. As expected, the positive chirp consistently leads to stable inversion probability which is considerably higher than for zero or negative chirp. Complete inversion is accomplished at the highest intensity with a rate of 98%. Surprisingly, as the linear frequency chirp rate c' becomes negative, the inversion probability increases to a value comparable to the rate on the positive chirp side. This new feature is clearly due to adiabatic inversion, which has noticeable effects on population inversion at large pulse duration and which is independent of the sign of the chirp. It is conceivable that as we extend the pulse duration further into the picosecond regime, the positive and negative chirps may lead to similar inversion

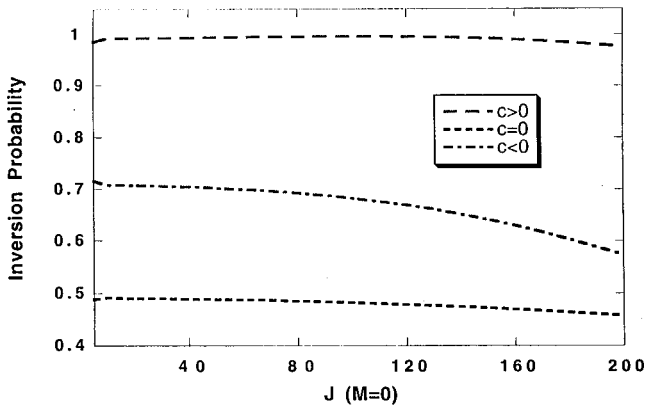

FIG. 11. Plot of the inversion probability of I_2 as a function of rotational quantum number J for $\tau=100$ fs, $E_0=19.5$ V/cm, and $\pm c'=5$ fs/cm^{-1}.

probability as the adiabatic effect dominates. In contrast, in the small chirp regime, vibrational coherence is the dominant effect. The large valley in the negative chirp regime clearly indicates intrapulse pump–dump mechanics. Also noticeable is the increase of the depth of the valley with field intensity, which indicates an increasingly efficient back transfer.

The absorption spectrum of I_2 spreads over more than one thousand wave numbers, which is larger than the bandwidth of the laser field used in this study. Consequently, a thermal distribution poses a major challenge to the complete inversion of I_2 with the chosen pulse bandwidth of 500 cm^{-1}. We examine in Fig. 11 the rotational number dependence of the inversion probability and find similar behavior to LiH. In fact, our results show that the inversion probability remains almost constant from $J=0$ to $J=100$.

Finally, the inversion probability is given in Fig. 12 as a function of temperature from 250 to 650 K for pulses of different durations. The chirps of these pulses are positive but with different values such that the pulse durations are 200, 300, and 400 fs for the given bandwidth of 500 cm^{-1}. Here, thermal distributions of vibrational and rotational states are included in the calculation through sampling of the initial states. Though there is a slight decrease in inversion probability as temperature increases, this dependence is rather weak and the probability remains nearly constant for the longest pulse duration of 400 fs. In comparison, the longest pulse is more sensitive to electronic dephasing.

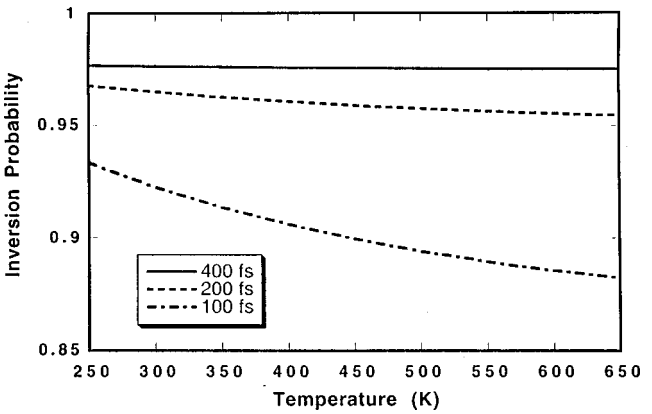

FIG. 12. Plot of the inversion probability of I_2 as a function of temperature for pulses of $\tau=100$, 200, and 400 fs with a fixed bandwidth of $\Gamma=500$ cm^{-1}.

IV. CONCLUSIONS

As a result of the analysis and calculations presented above, we have come to the intriguing conclusion that complete electronic state inversion of molecular systems can be achieved and sustained by virtue of introducing positive frequency modulation in intense broadband ultrafast light pulses. In summary, we rephrase the major findings from the previous sections.

(1) The prerequisite for complete population inversion is a broad pulse bandwidth comparable to the range of the absorption spectrum of interest, as required by Eq. (13). As suggested by the area relation for a transform-limited π pulse, we conclude that complete inversion requires intense femtosecond pulses, which may also induce multiphoton processes. Chirped pulses of the same bandwidth can significantly reduce the peak intensity by stretching the pulse duration, thus avoiding complications due to other possible high-intensity optical processes.

(2) Because of the vibrational coherence induced by femtosecond pulses, a positive chirp enhances population transfer by avoiding de-excitation, whereas a negative chirp suppresses population inversion by an intrapulse pump–dump mechanism, returning population to the ground state. With a sufficiently large positive chirp, the excited state population reaches saturation without Rabi oscillation. The saturation depends on the power spectrum; beyond a critical intensity, the inversion probability reaches a value of 99%, indicating complete inversion. Once beyond these critical values, the state of complete inversion is stable with respect to variations in pulse parameters such as the intensity, pulse duration, linear chirp rate, higher order frequency modulation (e.g., cubic and higher order chirps), and frequency offset within the absorption spectrum. Further, by taking account of rotational effects and thermal distribution, we find the above mechanism extremely robust for realistic molecular systems. Even in condensed phases, high inversion probabilities are sustained as long as the pulse duration does not substantially exceed the shortest relaxation time scale.

(3) At longer pulse durations, a different mechanism termed adiabatic frequency sweeping becomes important in population inversion. The adiabatic condition requires that the rate of sweeping, or equivalently the linear chirp rate, is sufficiently small compared to the Rabi frequency. Furthermore, complete inversion is only possible if the range of frequency sweep covers the entire frequency spectrum involved. Since the adiabatic effect is independent of the sign of the chirp, the negative chirp pulses become more effective than transform-limited pulses when the adiabatic effect overwhelms the vibra-

tional coherence effect. Therefore, we have $P_e(c>0) > P_e(c=0) > P_e(c<0)$ for femtosecond pulses and $P_e(c>0) > P_e(c<0) > P_e(c=0)$ for picosecond pulses. (P_e is the inversion probability defined as the excited electronic state population after the excitation of an initially ground state system.) In any case, a positively chirped pulse is always preferred.

As evident in this paper, as in other studies, frequency modulated laser pulses induce remarkable dynamic effects in molecular systems, which are impossible for transform-limited pulses. Even in the weak-response limit, the sign of the chirp proves crucial in wave packet focusing and defocusing.[28] In pump–dump and pump–probe experiments, the chirp of the second pulse can be optimized to follow the motion of the wave packet induced by the first laser pulse, and thus improve the quantum yield substantially.[29,15] The chirp also proves important for understanding intrapulse dynamics present in two-photon, three-photon, and multiphoton processes.[30,25] It has also been suggested that a chirped infrared laser may be used to transfer population to high vibrational overtones.[12] In the present study, we find that a positive chirp can significantly enhance population inversion and leads to essentially complete inversion. In conclusion, chirp-dependent effects allow us to explore the coherence between laser fields and molecular systems, especially in high-order and multiphoton processes, and to maximize the capability of laser-induced chemical selection and control.

With the help of feedback control and pulse shaping techniques, the fluorescence yield of dye molecules in solution and thus the population transferred to the excited state can be optimized automatically with no previous information being supplied about the solution.[9] The experimental outcome agrees with the present study and indicates that maximum excited state population is indeed produced by an intense, wide bandwidth, positively chirped pulse.

Many applications of molecular π pulses can be envisioned, including the preparation of pure samples of electronically excited molecules for further spectroscopic, scattering, and diffraction experiments,[31,32] more effective pumping of molecular lasers, brighter ultrafast pulse fluorescence microscopy, and induced transparency of matter.

APPENDIX: STOCHASTIC METHOD FOR SIMULATING PURE ELECTRONIC DEPHASING

Intuitively, pure electronic dephasing arises from random fluctuations of the relative phase between electronic surfaces. It then follows that electronic dephasing can be simulated numerically through the introduction of a random phase which satisfies certain stochastic conditions.[33] To be specific, consider the equation of motion for a two-state molecular system

$$i\hbar\dot{\psi}_e = \theta(t)\psi_e + \hat{H}_e\psi_e - i\Omega(t)\psi_g, \tag{A1}$$

$$i\hbar\dot{\psi}_g = \hat{H}_g\psi_g - i\Omega^*(t)\psi_e, \tag{A2}$$

where $\Omega(t)=\mu E(t)/\hbar$ is the Rabi frequency and ψ_g and ψ_e are the wave functions on the excited and ground surfaces, respectively. The random phase $\theta(t)$ is a stochastic Gaussian variable defined by

$$\langle\theta(t)\rangle = 0, \tag{A3}$$

and

$$\langle\theta(t)\theta(t')\rangle = \frac{1}{T_2}\delta(t-t'), \tag{A4}$$

where T_2 is the pure dephasing time. Because $\theta(t)$ is not an operator, it does not appear in the equation of motion for the diagonal terms ρ_e and ρ_g. For the off-diagonal term, we have

$$\begin{aligned}\rho_{eg}(t) &= \langle\psi_e(t)\psi_g^*(t)\rangle \\ &= \int_0^t \left\langle \exp\left[i\int_{t'}^t \theta(\tau)d\tau \right] \right\rangle G(t')dt' \\ &= \int_0^t e^{-(t-t')/T_2} G(t')dt', \end{aligned} \tag{A5}$$

where $G(t) = -i(\hat{H}_e\rho_{eg} - \rho_{eg}\hat{H}_g) - i(\Omega\rho_g - \Omega^*\rho_e)$. The integral form in Eq. (A5) can be easily reduced to the Bloch equation for the off-diagonal term ρ_{eg}. Thus, pure dephasing can be incorporated on the wave function level by introducing a random phase variable. This approach reduces the dimensionality required for calculating the density matrix by half via averaging the wave function over the random phase. Furthermore, the proposed numerical method is applicable to an arbitrary phase correlation function in Eq. (A4), which cannot be described by the Bloch equation of motion.

[1] S. A. Rice, Science **258**, 412 (1992).
[2] D. J. Tannor and S. A. Rice, J. Chem. Phys. **83**, 5013 (1985).
[3] W. S. Warren, H. Rabitz, and M. Dahleh, Science **259**, 1581 (1993).
[4] P. Brumer and M. Shapiro, Annu. Rev. Phys. Chem. **43**, 257 (1992).
[5] R. Kosloff, A. D. Hammerich, and D. J. Tannor, Phys. Rev. Lett. **69**, 2172 (1992).
[6] B. Kohler, V. V. Yakovlev, J. Che, J. L Krause, M. Messina, K. R. Wilson, N. Schwentner, R. M. Whitnell, and Y. J. Yan, Phys. Rev. Lett. **74**, 3360 (1995).
[7] B. Kohler, J. Krause, F. Raksi, K. R. Wilson, R. M. Whitnell, V. V. Yakovlev, and Y. J. Yan, Acc. Chem. Res. **28**, 133 (1995).
[8] J. Cao, M. Messina, and K. R. Wilson, J. Chem. Phys. **106**, 5239 (1997).
[9] C. J. Bardeen, V. V. Yakovlev, K. R. Wilson, S. D. Carpenter, P. M. Weber, and W. S. Warren, Chem. Phys. Lett. **280**, 151 (1997).
[10] L. Allen and J. H. Eberly, *Optical Resonance and Two-Level Atoms* (Dover, New York, 1987).
[11] U. Gaubatz, P. Rudecki, S. Schiemann, and K. Bergmann, J. Chem. Phys. **92**, 5363 (1990).
[12] S. Chelkowski, A. Bandrauk, and P. B. Corkum, Phys. Rev. Lett. **65**, 2355 (1990).
[13] J. S. Melinger, A. Hariharan, S. R. Gandhi, and W. S. Warren, J. Chem. Phys. **95**, 2210 (1991).
[14] S. Schiemann, A. Kuhn, S. Steuerwald, and K. Bergmann, Phys. Rev. Lett. **71**, 3637 (1993).
[15] J. Cao and K. R. Wilson, J. Chem. Phys. **106**, 5062 (1996).
[16] M. N. Kobrak and S. A. Rice, Phys. Rev. A **57**, 1158 (1998).
[17] S. Ruhman and R. Kosloff, J. Opt. Soc. Am. B **7**, 1748 (1990).
[18] G. Cerullo, C. J. Bardeen, Q. Wang, and C. V. Shank, Chem. Phys. Lett. **262**, 362 (1996).
[19] J. Cao, C. Bardeen, and K. R. Wilson, Phys. Rev. Lett. **80**, 1406 (1998).
[20] J. Somlói and A. Lörincz, Phys. Rev. A **43**, 2397 (1991).
[21] B. Amstrup, A. Lörincz, and S. A. Rice, J. Phys. Chem. **97**, 6175 (1993).
[22] L. Shen and H. Rabitz, J. Chem. Phys. **100**, 4811 (1994).

[23] M. Holthaus and B. Just, Phys. Rev. A **49**, 1950 (1994).
[24] J. A. Cina and T. J. Smith, J. Chem. Phys. **98**, 9211 (1993).
[25] J. Cao, J. Che, and K. R. Wilson, J. Phys. Chem. **102**, 4248 (1999).
[26] H. Partridge and S. R. Langloff, J. Chem. Phys. **74**, 2361 (1980).
[27] Various units have been used for c', for example, $1/cm^{-2}$, fs/cm^{-1}, and fs^2, depending on whether ω and ω_0 in Eq. (3) are in units of cm^{-1}, fs^{-1}, or a mixed notation.
[28] C. J. Bardeen, J. Che, V. V. Yakovlev, K. R. Wilson, V. A. Apkarian, C. C. Martens, R. Zadoyan, B. Kohler, and M. Messina, J. Chem. Phys. **106**, 8486 (1997).
[29] M. Sterling, R. Zadoyan, and V. A. Apkarian, J. Chem. Phys. **104**, 6497 (1996).
[30] V. V. Yakovlev, C. J. Bardeen, J. Che, J. Cao, and K. R. Wilson, J. Chem. Phys. **108**, 2309 (1998).
[31] M. Ben-Nun, J. Cao, and K. R. Wilson, J. Phys. Chem. **101**, 8743 (1997).
[32] J. Cao and K. R. Wilson, J. Phys. Chem. **102**, 9523 (1999).
[33] P. Gross, D. Neuhauser, and H. Rabitz, J. Chem. Phys. **98**, 9650 (1993).